VISUALIZAION OF AUTO-IGNITION PHENOMENON UNDER THE CONTROLED BURST PRESSURE

Yamashita, K.[1], Saburi, T.[2], Wada, Y.[2], Asahara, M.[1], Mogi, T.[3], and Hayashi, A.K.[1]
[1] Graduate School of Science and Engineering, Aoyama Gakuin University, 5-10-1 Fuchinobe, Chuo-ku, Sagamihara-shi, Kanagawa 252-0206, Japan
[2] Research Institute of Science for Safety and Sustainability, National Institute of Advanced Industrial Science and Technology, 16-1 Onogawa, Tsukuba-shj, Ibaraki 305-8569, Japan
[3] Graduate School of Engineering, The University of Tokyo, 7-3-1 Hongo, Bunkyo-ku, Tokyo 113-8656, Japan
Corresponding Author: Saburi, T., t.saburi@aist.go.jp

ABSTRACT

High-pressure hydrogen jet released into the air has a possibility to ignite in a tube without any ignition source. The mechanism of this "auto-ignition" is considered that a shock wave produced after a diaphragm rupture causes the ignition by a heat up of the mixing region. In these years, flow visualization study for the auto-ignition process has been started to conduct to understand its detailed mechanism, but such ignition still has not be known well. This study deals with a observation of the auto-ignition phenomena in the rectangular tube. The results show that a flame is confirmed when the shock wave pressure reaches 1.2-1.5 MPa at the wall and that the ignition occurs near the wall, then multiple ignitions come out while the shock wave propagates and they become a flame.

1.0 INTRODUCTION

High-pressure hydrogen is released from a rupture disk through the pipe into the air as an emergency action in hydrogen station and chemical plant. While this process, the high-pressure hydrogen may spontaneously and automatically ignite to yield a flame propagating without any ignition source. This "auto-ignition" is not caused by ignition source but caused by the diffusion flow and was experimentally confirmed by Wolanski et al [1]. However its detailed ignition mechanism in the tube has not been well clarified yet. It is necessary to define a safety criteria preventing the flame development when the high-pressure hydrogen is accidentally released at hydrogen station and chemical plant. A clarification of detailed auto-ignition process is expected from these back ground.

A variety of experimental and numerical studies have been conducted on this field. Shock tube experimental system equipped with a diaphragm to release hydrogen by a rupture disk is generally used to study hydrogen auto-ignition phenomenon. The ignition possibility of a hydrogen jet due to a sudden release depends on the burst pressure of diaphragm and tube geometry [2], [3] [4], [5]. The burst pressure that is enough to cause auto-ignition becomes lower with increasing tube length to a certain size, but it becomes higher with further tube extension [5]. The tube geometry downstream from the diaphragm affects the ignition behaviour, but that upstream from the diaphragm does not affect it [2], although the configuration of the tube and connectors may affect the gas dynamics downstream. Variation of the diaphragm rupture behaviours such as a rupture speed and its behaviour [6] due to diaphragm position, diaphragm shape, diaphragm materials causes some difference in the ignition possibility [7], [8], [9]. The flame structure and flammable range outside the tube have been visualized by experiments [3], [5], [10] and numerical simulations [4], [7]. The ignition process in the tube has been numerically simulated [7], [8], [11], [12], [13], and it has also been visualized by experimental studies in these years [14]. However, there is a question for the quantitative discussion because some of the experimental studies have a lack of reproducibility due to inaccuracy of the rupture process and the rupture pressure. In particular, there are only a few results of the visualization of the phenomenon in the tube.

In this study, a shock tube experiment was examined to make clear the ignition and flame forming process of high-pressure hydrogen flow in the tube. A circular shock tube apparatus is equipped with a plunger system to control the burst pressure, a circular-to-rectangular conversion flange to

restrain discontinuous cross-section change and a rectangular tube with glass windows for optical observation. Two high-speed cameras are used to take a shadowgraph photograph and a direct photograph simultaneously.

2.0 EXPERIMENTAL SET UP

The experimental apparatus is based on the shock tube system that consists of high-pressure hydrogen region and ambient pressure air region (Figure 1) separated by a diaphragm. The diaphragm made of PET film (Melinex, Teijin DuPont) keeps hydrogen region at high-pressure. The thickness of the PET film is adjusted according to the burst pressure to expect that the film fails and ruptures at predetermined pressure, but the thickness-based rupture control is generally insufficient in its accuracy. Then, a plunger system is introduced this time. It is composed of a barrel with a solenoid coil, a tungsten needle positioned at the coil end, and a step-up circuit, and is mounted diagonally to high-pressure side of the diaphragm flange. When the step-up circuit is switched on, a large pulsed current flows through the coil and it forms a magnetic field along the barrel. The magnetic force pulls and accelerates the tungsten needle. The needle flights along barrel, and hits and ruptures the diaphragm. The plunger system is able to rupture the diaphragm precisely by pressure base control, and the pressure is measured using a strain gage pressure transducer (PHA-L-20MP, Kyowa Electronic Instruments). The rectangular test section equipped with silica glass windows and sensors is connected to the tube end in the ambient pressure section. The high-pressure hydrogen propagation and ignition and flammable behaviours are observed by high-speed cameras through the windows, and pressure and luminescence histories are recorded at 30mm intervals using the pressure sensors (PCB M111A24, Piezotronics Inc.) and light detectors (PDA25K, Thorlabs), respectively. When the step-up circuit switch is on, the trigger signal is sent to start recording on a data logger and high-speed cameras. Two high-speed cameras record the shadowgraph system to visualize density gradient and the direct flame images, respectively. Regarding to an optics setup for shadowgraph system, illumination source is a xenon lamp (LS-75, KATOKOKEN) and the reflected and collimated light off a schlieren mirror passes through the windows of the measurement section and the image passes through a Fresnel lens and focus on the first shadowgraph camera positioned normal to the glass window. The flame dynamics are directly captured using the second camera positioned slightly oblique to the window. The cross-section dimension of the rectangular tube originally at ambient pressure is 10 mm × 10 mm and the length of that ranges from 200 mm to 800 mm. The circular-to-rectangular conversion flange connects between the circular high-pressure section and rectangular ambient pressure section changing gradually from circle to rectangle in a 20 mm length to avoid such sudden shape of the cross-section.

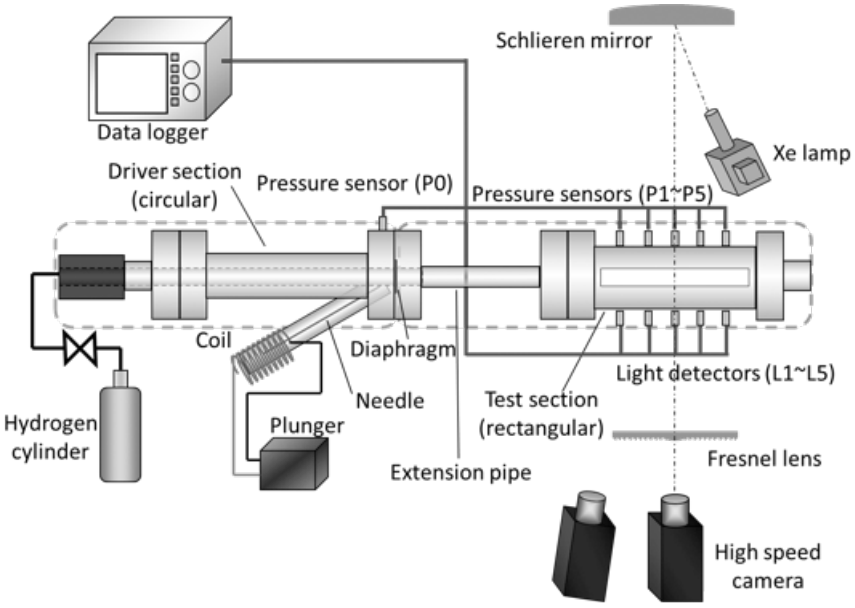

Figure 1. Experimental schematic of whole system; Orange and blue broken lines respectively mean driver (high pressure) circular section and test (ambient pressure) rectangular section.

3.0 RESULTS AND DISSCUSION

The Experimental study is conducted for the auto-ignition of high pressure hydrogen injection into the tube in the present study. First of all we compare the shock wave (pressure wave) velocities with the burst pressure among the passed studies [3,5] and the present one. Secondly we show the pressure profiles for the different burst pressures. And thirdly the observation of auto-ignition and flame propagation in the tube are performed using a high speed camera.

3.1 Shock wave velocities among the past studies, the present one, and the theory

The experimental shock wave velocities calculated from the arrival times between the sensors are compared with the theory and the past studies in Figure 2. The theoretical values are calculated from the following equation:

$$C_s = a_1 \sqrt{\frac{\gamma - 1}{2\gamma} + \frac{\gamma + 1}{2\gamma} \frac{p_2}{p_1}}$$

Where C_s – theoretical shock speed, m/s; a – sound speed, m/s; γ – specific heat ratio; subscript 1 and 2 – condition ahead of the shock and behind the shock, respectively. The shock wave decays while its propagation, but the degree of the decay is sufficiently small in the tube length of 1 m [5]. The experimental shock velocity in the present study increases as the burst pressure increases, and the increase in the shock wave velocity becomes slower when the burst pressure increases. The results of the present experimental shock wave velocities agree with the theory and the past studies [3, 5]. The present experimental data remain at 80–90 % of the theoretical one and the past studies also shows similar results. For the possible causes of the deviation of the experimental results from the theory, it is considered that there are the boundary layer effect, finite time of rupture process, and three-dimensional effect.

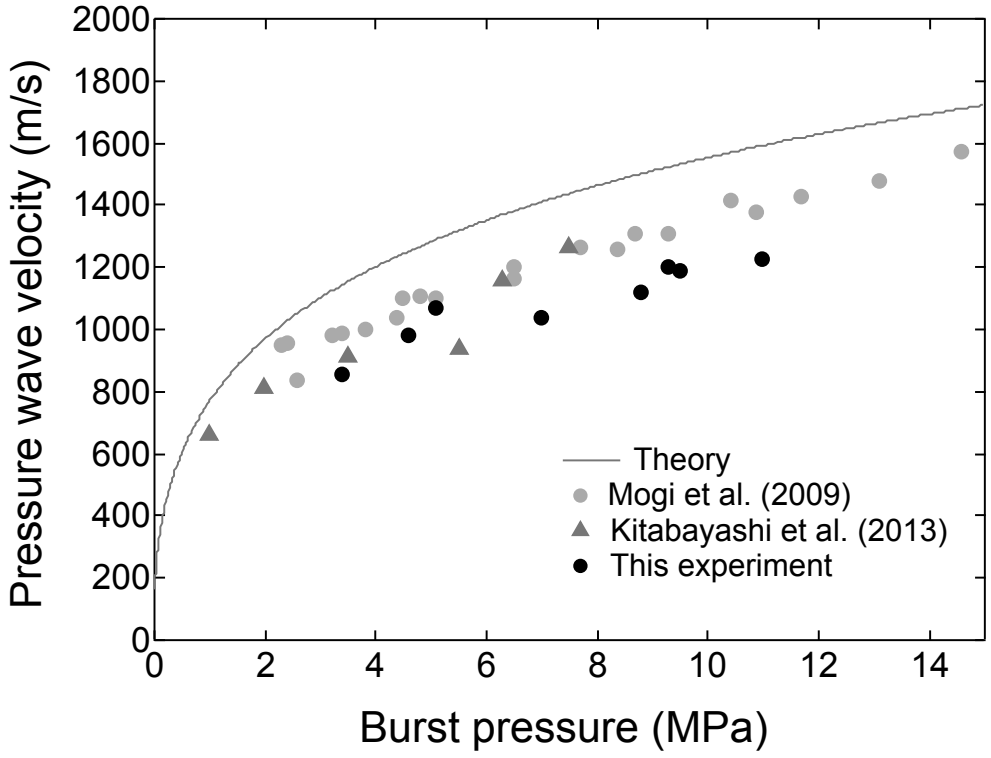

Figure 2. Pressure wave velocity comparison between the theory and experimental results for a tube

3.2 Sensors measurement for auto-ignition determination

The pressure history by pressure gauges and emission history by light sensors are compared to figure out whether auto-ignition occurs or not. The time histories for the case of no-ignition (the burst pressure of 5.1 MPa), the ignition case occurred in the measurement section (the burst pressure of 9.5 MPa), and the ignition case occurred before the measurement section (the burst pressure of 10 MPa), are shown in Figures 3.1, 3.2, and 3.3, respectively. In the captions of the figures, P1 – P5, L1 – L5, and the values in mm, are the pressure sensors, the light sensors, the distance from the diaphragm at each sensor, respectively. It should be mentioned that the sensor L1 detects no useful data due to the sensor failure in the experiments. Additionally the time $t = 0$ does not imply the diaphragm ruptured time, but the trigger time. Generally, pressure suddenly rises up on the arrival of the shock wave and emission is detected on the flame passing through the sensor position. For the case of no-ignition as shown in Figure 3.1, a sudden pressure rise by the shock wave reaches about 1 MPa and no emission is detected. For the case of ignition occurred in the measurement section as shown in Figure 3.2, the first pressure rise reaches approximately 1.5 MPa at P3, P4, and P5, and emission from the flame is also detected at L3, L4, and L5. On the other hand, the pressure rise reaches 1.2 MPa at P2, and no flame emission is detected at L2. There are the sensor positions just before the L3 position where the flame is detected. Finally for the case of ignition occurred before the measurement section as shown in Figure 3.3, all pressure sensors detect more than 1.5MPa at the first pressure rise and all workable light sensors detect flame emission. Therefore ignition should take place when the wall pressure reaches 1.2–1.5 MPa considering from these three cases. In addition, each light sensor detects emission from the flame during about 100 μs, which indicates that the length of flame region corresponds to 10 cm if the flame propagates at the same order of the shock wave velocity. It should be mentioned that the bust pressure in the case of ignition is observed relatively higher than past similar studies. It comes from the difference in the tube configuration such as the cross-sectional area that the smaller cross-sectional area gives ignition with the smaller burst pressure [2], [3], [4].

The experimental results of hydrogen ignition by Dryer et al. [2] show that the ignition is observed at the storage pressure of 2 MPa, that by Golub et al. [4] is at the storage pressure of 4-9 MPa, and the present study shows the ignition occurs at the storage pressure higher than 4 up to 11 MPa. The reason for such difference is that first of all, as imagine at the experiments by Dryer et al. [2], there might be a small step between a tube and connector, which gives a ignition. The results by Golub et al. [4] and that by the present study have a similar ignition storage pressure, which is between 4 and 9 MPa. Hence the experiment by Golub et al. [4] and the present ones have the similar accuracy for the experimental tube and measurement system.

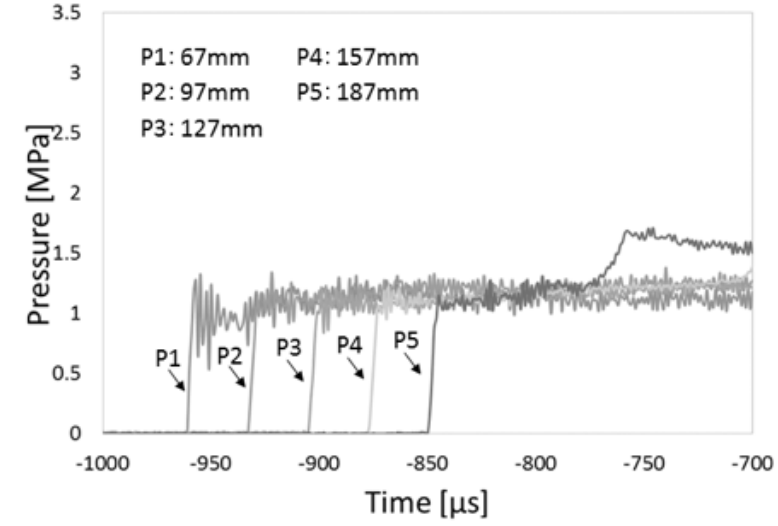

Figure 3.1 Pressure histories at the tube wall for 5.1 MPa of the burst pressure (no-ignition case) : P1-P5 are the pressure sensors and the numbers in mm are the distance from the diaphragm.

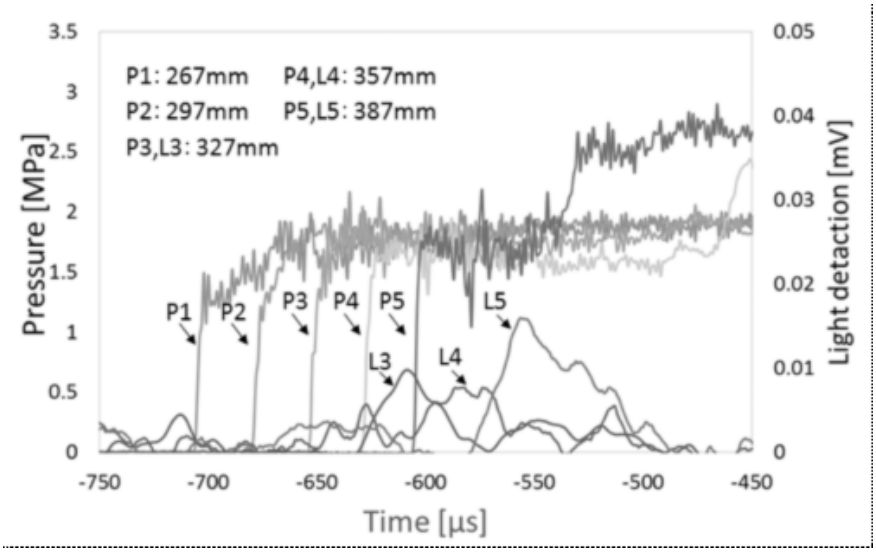

Figure 3.2. Pressure and emission histories at the tube wall for 9.5 MPa of the burst pressure (the ignition case in the measurement section) : P1-P5 are the pressure sensors, L3-L5 are the light sensors, and the numbers in mm are the distance from the diaphragm.

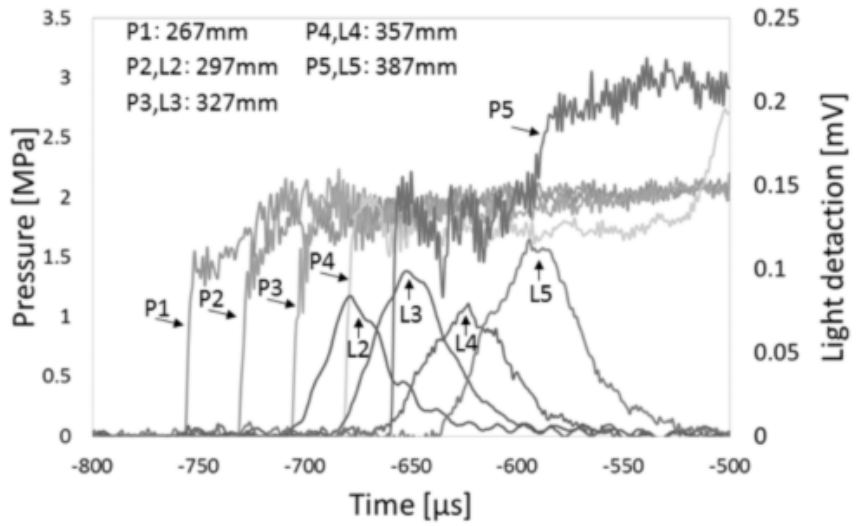

Figure 3.3. Pressure and emission histories at the tube wall for 10.0 MPa of the burst pressure (ignition before the measurement section) : P1-P5 are the pressure sensors, L2-L5 are the light sensors, and the numbers in mm are the distance from the diaphragm.

3.3 Observation of ignition phenomenon in the tube

The shadowgraph and direct images taken from the case of ignition near the measurement section in the tube are illustrated in Figure 4.1 and Figure 4.2, respectively. Some notes are described below before discussion;

- These images are taken from the different experimental condition (the burst pressure is 9 MPa) from the previous paragraph.
- The time t=0 indicates the arrival time of the shock at the measurement section.
- Lines in the shadowgraph images illustrate the shock wave, the flame front, the flame tale, and the hydrogen jet.
- As mentioned in the section 2, the camera for the shadowgraph system is installed normal to the glass window and the camera for the direct photography is set to the window with a little angle. Therefore the situation gives the scale difference between two images and the reflected lights (160 and 170 μs in Figure 4.2) come out at right side of the direct images.

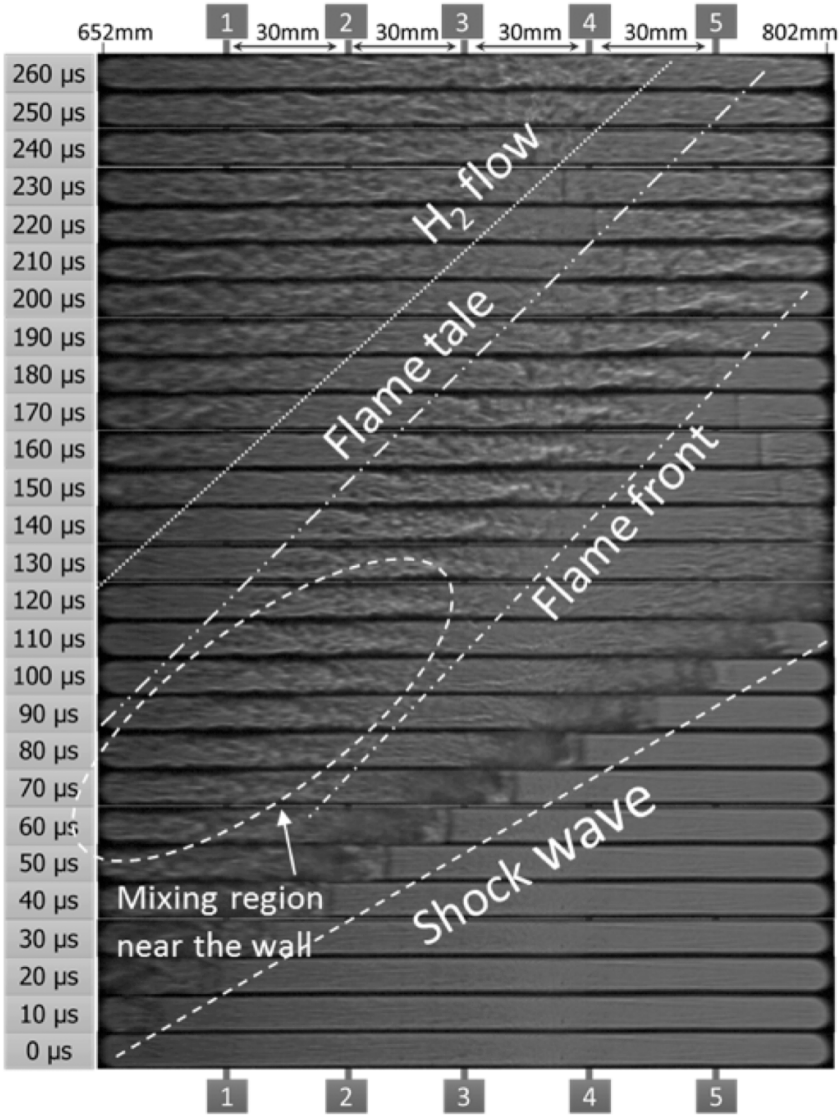

Figure 4.1. Shadowgraph photograph for 9.0 MPa of burst pressure

For the shadowgraph picture, the shock wave enters the measurement section at first, the high-density fluctuation region corresponding to a mixed region propagates subsequently, and then the hydrogen jet follows the precursor shock wave and the mixed region. The mixed region is divided into two parts; one propagating subsequent to the precursor shock wave and another accompanying the shock wave at around 70 μs. For the part of mixture region accompanying the shock wave, the flame becomes weak as it propagates, and it seems to disappear as seen in Figure 4.2. On the other hand, the part of mixture region subsequent to the shock wave seems to correspond to the propagating flame shown in Figure 4.2. The higher density gradient is observed near the wall in the subsequent mixed region. This high-density gradient region may be generated by the fluid dynamic instability which is confirmed in the numerical simulations [5], [7], [11], [12].

In Figure 4.2, a flame kernel seems to arise from the ignition that appears near the wall at 60 μs. Another flame kernel comes out from the other side of the wall at 70 μs and gradually expands as it propagates. Further, new flame kernels take place everywhere around 130–150 μs. Finally those flames combine together to form the large flame region over the tube width. The position of the first-appeared flame kernel corresponds to the high mixed region near the wall in the shadowgraph images.

It indicates that the ignition first takes place at the mixed region near the wall, and the same trend is confirmed in the other experimental study [14]. Additionally, the ignition occurs at many places and their flames merge together to form the flame region. The length of the whole flame region reaches around 10 cm measured by the direct images, and this is almost the same length to that obtained from the light sensors measurement. The flame length evaluated by the light sensors and that measured by the photo images are consistent with each other.

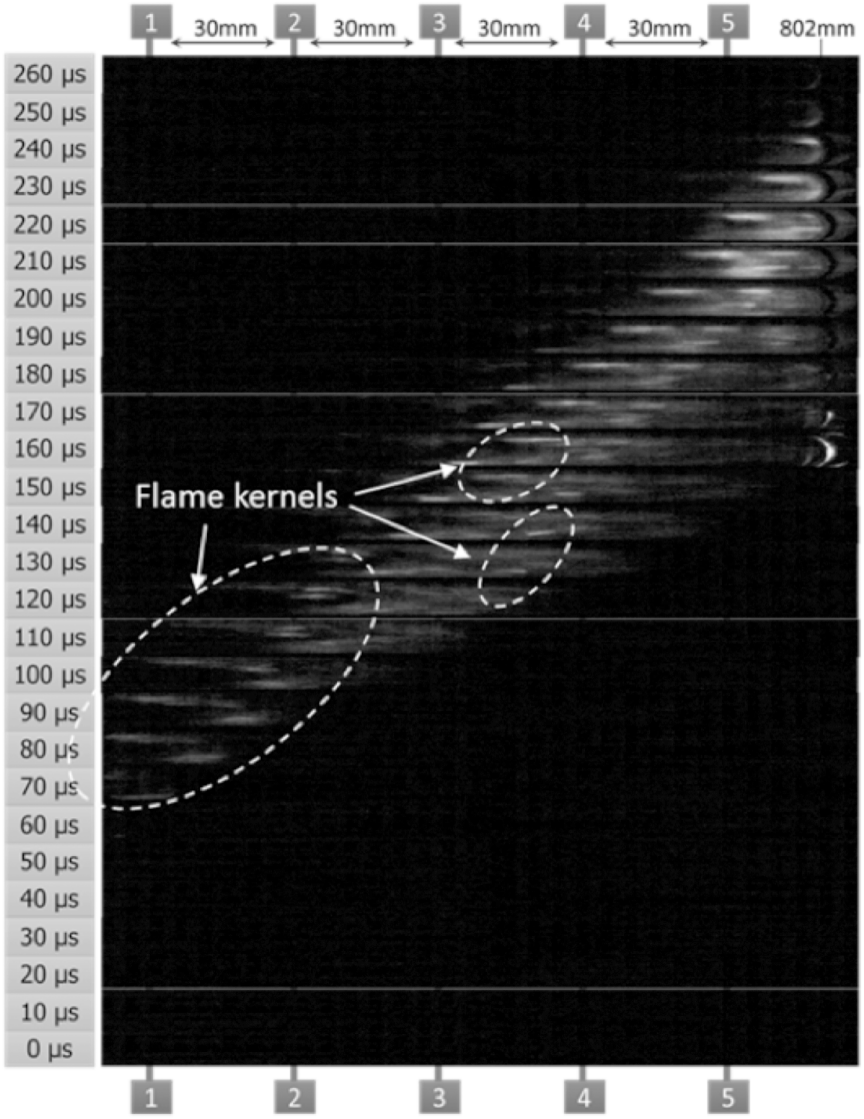

Figure 4.2. Direct photograph for 9.0 MPa of burst pressure

4.0 CONCLUSION

The followings are obtained from the present study of the experimental investigation of the shock wave and the flame in the shock tube using the pressure and light sensor measurements and the observations by the high-speed camera photography.

- The emission from the Flame is confirmed when the shock wave pressure reaches 1.2–1.5 MPa at the wall.
- The ignition takes place in the mixed region near the wall at first, multiple ignitions occurs as the shock propagates, then they form the flame region. This is consistent with the past study [15].
- The ignition requires sustenance of the mixed region as long as the local ignition delay time.

From these findings, it's important to keep the shock wave pressure not to reach ignition requiring pressure in order to prevent auto-ignition for high pressure hydrogen discharge process. Ignition possibility can be reduced by controlling the temperature near the outlet. Furthermore, the auto-ignition limit is generally discussed by using the auto-ignition curve that is specified the tube length and the burst pressure as parameters in the past studies. It is suggested that using the parameter based on shock wave quantity is more appropriate since they are including ambient condition. This ambient condition dependency on shock wave strength is not discussed in the present paper.

REFERENCES

1. Wolański, P. S. and Wójcicki, S., Investigation into the Mechanism of the Diffusion Ignition of a Combustible Gas Flowing into an Oxidizing Atmosphere, *Proceedings of the Combustion Institute*, **14**, 1973, pp. 1217-1223.
2. Dryer, F.L., Chaos, M., Zhao, Z., Stein, J.N., Alpert, J.Y. and Homer, C.J., Spontaneous Ignition of Pressurized Release of Hydrogen and Natural Gas into Air, *Combustion Science and Technology*, **179**, Issue 4-6 2007, pp. 663-694.
3. Mogi, T., Wada, Y., Ogata, Y. and Hayashi, A. K., Self-ignition and Flame Propagation of High-pressure Hydrogen Jet during Sudden Discharge from a Pipe, *International Journal of Hydrogen Energy*, **34**, Issue 14 2009, pp. 5810-5816.
4. Golub, V.V., Baklanov, D.I., Bazhenova, T.V., Golovastov, S.V., Ivanov, M.F., Laskin, I.N., Semin, N.V. and Volodin, V.V., Experimental and Numerical Investigation of Hydrogen Gas Auto-ignition, *International Journal of Hydrogen Energy*, **34**, Issue 14 2009, pp. 5946-5953.
5. Kitabayashi, N, Wada, Y., Mogi, T., Saburi and T., Hayashi, A. K., Experimental Study on High Pressure Hydrogen Jets Coming out of Tubes of 0.1–4.2 m in length, *International Journal of Hydrogen Energy*, **38**, Issue 19 2013, pp. 8100-8107.
6. Golovastv, S. and Bocharnikov, V., The influence of diaphragm rupture rate on spontaneous self ignition of pressurezed hydrogen: Experimental Investigation, *International Journal of Hydrogen Energy*, **37**, Issue 14, 2012, pp.10956-10962.
7. Wen, J.X., Xu, B.P. and Tam, V.H.Y., Numerical Study on Spontaneous Ignition of Pressurized Hydrogen Release through a Length of Tube, *Combustion and Flame*, **156**, Issue 11 2009, pp. 2173-2189.
8. Lee, H. J., Park, J.H, Kim, S.D, Kim, S. and Jeung, I. S., Numerical Study on the Spontaneous-ignition Features of High-pressure Hydrogen released through a Tube with Burst Conditions, *Proceedings of the Combustion Institute*, **35**, Issue 2 2015, pp. 2173-2180.
9. Golovastov, S. and Bocharnikov, V., The Influence of Diaphragm Rupture Rate on Spontaneous Self-ignition of Pressurized Hydrogen: Experimental Investigation, *International Journal of Hydrogen Energy*, **37**, Issue 14 2012, pp. 10956-10962.
10. Kim, S., Lee, H. J., Park, J.H. and Jeung, I. S., Effects of a Wall on the Self-ignition Patterns and Flame Propagation of High-pressure Hydrogen Release through a Tube, *Proceedings of the Combustion Institute*, **34**, Issue 2 2013, pp. 2049-2056.
11. Yamada, E., Watanabe, S., Hayashi, A. K., and Tsuboi, N., Numerical Analysis on Auto-ignition of a High Pressure Hydrogen Jet Spouting from a Tube, *Proceedings of the Combustion Institute*, **32**, Issue 2 2009, pp. 2363-2369.
12. Asahara, M., Yokoyama, A., and Hayashi, A.K., Numerical Simulation of Auto-ignition Induced by High-pressure Hydrogen Release with Detailed Reaction Model: Fluid Dynamic Effect by Diaphragm Shape and Boundary Layer, *International Journal of Hydrogen Energy*, **39**, Issue 35 2014, pp. 20378-20387.

13. Bragin, M. V., Makarov, D. V., Molkov, V.V., Pressure Limit of Hydrogen Spontaneous Ignition in a T-shaped Channel, *International Journal of Hydrogen Energy*, **38**, Issue 19, 2013, pp. 8039-8052.
14. Kim, Y.R., Lee, H. J., Kim, S. and Jeung, I. S., A Flow Visualization Study on Self-Ignition of High Pressure Hydrogen Gas Released into a Tube, *Proceedings of the Combustion Institute*, **34**, Issue 2 2013, pp. 2057-2064.
15. Bragin, M. V., Molkov, V.V., Physics of spontaneous ignition of high-pressure hydrogen released and transition to jet fire, *Inter national Journal of Hydrogen Energy*, **36**, Issue 3, 2011, pp. 2589-2596.